The Holocene 15,8 (2005) pp. 1172–1183

Palaeohydrology of the Southwest Yukon Territory, Canada, based on multiproxy analyses of lake sediment cores from a depth transect

Lesleigh Anderson,[1]* Mark B. Abbott,[2] Bruce P. Finney[3] and Mary E. Edwards[4]

([1]Department of Geosciences, University of Massachusetts Amherst, Amherst MA 01003, USA; [2]Department of Geology and Planetary Science, University of Pittsburgh, Pittsburgh PA 15260-3332, USA; [3]Institute of Marine Science, University of Alaska Fairbanks, Fairbanks AK 99775, USA; [4]Institute of Arctic Biology, University of Alaska Fairbanks and School of Geography, University of Southampton, Highfield, Southampton SO17 1BJ, UK)

Received 5 August 2003; revised manuscript accepted 22 April 2005

A HOLOCENE RESEARCH PAPER

Abstract: Lake-level variations at Marcella Lake, a small, hydrologically closed lake in the southwestern Yukon Territory, document changes in effective moisture since the early Holocene. Former water levels, driven by regional palaeohydrology, were reconstructed by multiproxy analyses of sediment cores from four sites spanning shallow to deep water. Marcella Lake today is thermally stratified, being protected from wind by its position in a depression. It is alkaline and undergoes bio-induced calcification. Relative accumulations of calcium carbonate and organic matter at the sediment–water interface depend on the location of the depositional site relative to the thermocline. We relate lake-level fluctuations to down-core stratigraphic variations in composition, geochemistry, sedimentary structures and to the occurrence of unconformities in four cores based on observations of modern limnology and sedimentation processes. Twenty-four AMS radiocarbon dates on macrofossils and pollen provide the lake-level chronology. Prior to 10 000 cal. BP water levels were low, but then they rose to 3 to 4 m below modern levels. Between 7500 and 5000 cal. BP water levels were 5 to 6 m below modern but rose by 4000 cal. BP. Between 4000 and 2000 cal. BP they were higher than modern. During the last 2000 years, water levels were either near or 1 to 2 m below modern levels. Marcella Lake water-level fluctuations correspond with previously documented palaeoenvironmental and palaeoclimatic changes and provide new, independent effective moisture information. The improved geochronology and quantitative water-level estimates are a framework for more detailed studies in the southwest Yukon.

Key words: Lake-level, effective moisture, palaeoclimate, palaeolimnology, carbon isotopes, nitrogen isotopes, Yukon Territory, Canada, Holocene.

Introduction

Previous palaeoecological studies in the semi-arid regions of central Alaska and southwest Yukon have identified long-term millennial-scale climatic fluctuations since the late Pleistocene (Cwynar, 1988; Stuart *et al.*, 1989; Cwynar and Spear, 1991; Wang and Geurts, 1991; Anderson and Brubaker, 1994; Edwards and Barker, 1994; Lacourse and Gajewski, 2000). Little is known, however, about the relative importance of temperature and effective moisture during the Holocene, or about quantitative changes in effective moisture (Ritchie and Harrison, 1993; Barber and Finney, 2000; Abbott *et al.*, 2000). Lake-level records provide a direct means to determine regional effective moisture because they reflect the water-table, which is controlled by effective moisture. In central Alaska, lake-level records from Birch Lake (Figure 1) provide evidence

*Author for correspondence (Present address: U.S. Geological Survey, Box 25046 MS-980, Federal Center, Denver CO 80225-0046, USA. E-mail: land@usgs.gov)

 10.1191/0959683605hl889rp

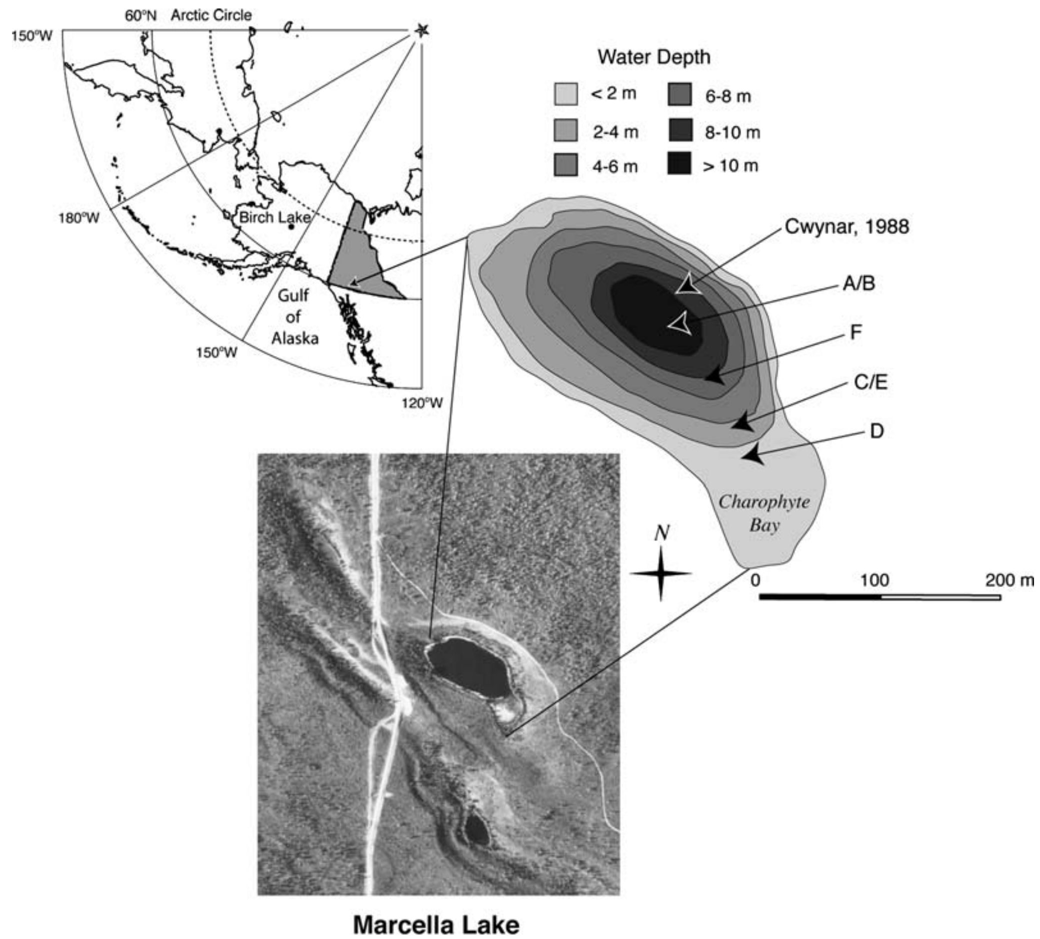

Figure 1 Location of the Yukon Territory, Marcella Lake and Birch Lake (modified from the Atlas of Canada, Natural Resources Canada) indicating core locations for this study and that of Cwynar (1988). (Photograph A22408, copyright 1949 by Her Majesty the Queen in Right of Canada, reproduced from the collection of the National Air Photo Library, with permission of Natural Resources Canada)

for effective moisture during the late Pleistocene and early Holocene (Barber and Finney, 2000; Abbott *et al.*, 2000; Finney *et al.*, 2000). Birch Lake was either seasonally dry or desiccated prior to 14 000 cal. BP. It subsequently filled, but levels fluctuated between 13 000 and 9000 cal. BP. Soon after 5500 cal. BP it overflowed, which is broadly coincident with oxygen isotope evidence for a transition to cooler and wetter climatic conditions in the central Brooks Range of northern Alaska (Anderson *et al.*, 2001). However, once overflowing, the lake was no longer sensitive to further increases in effective moisture and the late Holocene record is largely unknown. Less information is known about postglacial effective moisture variability in the southwest Yukon (Ritchie and Harrison, 1993). Previous studies have documented early Holocene warmth in the northern Yukon (Ritchie *et al.*, 1983; Burn 1997), and a middle-Holocene wet phase in the central Yukon (Pienitz *et al.*, 2000). Late-Holocene glacial advances occurred in the southwest Yukon, interpreted as evidence for cooler temperatures (Denton and Karlén, 1977; Calkin *et al.*, 2001)

This paper presents new evidence for lake-level variations in the southwest Yukon. Modern limnology and surface sediment data from Marcella Lake were used to develop a sedimentary model for shallow, intermediate and deep-water sites. During summer the lake is thermally stratified and surface-sediment composition variations are controlled by thermocline depth. Assuming that lake-level changes adjust thermocline depths, variations in surface sediment composition at different water depths record lake-level variations through time (e.g., Digerfeldt, 1986). Following this approach, we reconstructed a quantitative lake-level record from variations in sediment cores along a gently sloping bathymetric profile. The sampling resolution and sediment core chronologies are of sufficient quality to document the timing of effective moisture shifts at the millennial scale, or better.

Field area

Marcella Lake (60.074°N, 133.808°W, 697 m a.s.l.) is located in a northwest to southeast trending depression on a terrace of unconsolidated till and outwash east of the Lubbock River in the southern Yukon Plateau physiographic region (Figure 1). The larger depression is interpreted as a former melt-water channel that presumably formed $\sim$11 000 cal. BP during recession of the northern edge of the Cordilleran Ice Sheet (Dyke *et al.*, 2002). The lake is small (0.4 km^2), shallow (9.7 m) and sits $\sim$20 m below the terrace surface in a well-defined 0.8-km^2 watershed. Surface inflow is limited to the local basin and outflow appears to be restricted to evaporation. Bathymetry is simple with a gently dipping slope from the shallow southeast bay to the deepest area of the basin (Figure 1). The watershed is dominated by open stands of lodgepole pine (*Pinus contorta*), trembling aspen (*Populus tremuloides*) and white spruce (*Picea glauca*). Sage (mainly *Artemisia frigida*) and grasses (*Poaceae*) grow on treeless well-drained south-facing slopes. Submerged charophyte vegetation dominates the southeast bay. Otherwise, littoral plant communities are diverse, but limited to shallow near-shore areas. Water levels today reflect water-table depth.

Marcella Lake is located ~200 km northeast of the Gulf of Alaska in a pronounced rain shadow of the St Elias Mountains, restricting mean annual precipitation in the interior to ~260 mm/yr (Wahl *et al.*, 1987). The intensity and position of the Aleutian Low, centred over the Gulf of Alaska, influences the trajectory and intensity of storms entering the region. A precipitation maximum occurs between May and September (Wahl *et al.*, 1987; Mock *et al.*, 1998). Mean annual temperatures measured at nearby Teslin and Whitehorse are between −2 and 0°C. January mean temperatures range between −15 and −20°C and July mean temperatures are between 10 and 15°C (Wahl *et al.*, 1987; Environment Canada, 2003). Regional lake-ice break-up occurs between April and May and freeze-up occurs between October and November. Cwynar (1988) produced a detailed late-Quaternary pollen record for this site; in his study the lake was called Kettlehole Pond.

Limnology and sedimentation

Limnological measurements made in July 2000 provide a basis for understanding the controls on modern sedimentary facies and a means to interpret down-core sedimentary facies changes in terms of lake level. Autocthonous sedimentation of bio-induced calcium carbonate and organic matter are predominant throughout the lake. The wind-protected basin experiences a strong thermal stratification, which is shown by temperature and dissolved oxygen profiles of the water column (Figure 2). Surface-water was 16.3°C, a thermocline occurred between 5 and 8 m depth and bottom water temperatures were 5.5°C. Dissolved oxygen concentrations at the surface, 9.2 mg/L, decreased to <0.3 mg/L in the hypolimnion. However, intact surface sediments from gravity cores taken in 9.6 m depth clearly showed the sediments to be bioturbated. The lake probably overturns at least once, but more likely twice per year during the spring and/or autumn.

Thermocline depth is controlled by lake volume and heat capacity, and is strongly influenced by lake level (e.g., Fee *et al.*, 1996). In general, for lakes with simple bathymetry, an increase in lake volume will result in a decrease in thermocline depth and *vice versa*. Marcella Lake basin morphometry is simple and has been modified very little by Holocene sedimentary infilling. If past thermoclines formed at depths similar to today (~5–8 m), then contrasting sedimentation above and below the thermocline provides a means to reconstruct former lake levels from sediment cores from shallow-to-deep depths.

Marcella Lake water alkalinity, calcium and magnesium concentrations (339 mg $CaCO_3$/L, 25.4 mg/L Ca^{2+} and 70.8 mg/L Mg^{2+}) sustain bio-induced carbonate precipitation within surface waters by Charophytes (*Chara* sp.) in the shallow southeast bay (McConnaughy, 1991; McConnaughy *et al.*, 1994). Randomly collected surface sediments (collected by L.C. Cwynar) demonstrate how relative proportions of calcium carbonate and organic matter are related to thermocline depth (Figure 2). In general, sediments accumulating above the thermocline (≤5 m) contain significantly more calcium carbonate (30–80%) than organic matter (20–50%). Sediments accumulating within the upper-thermocline (5–6 m) contain approximately equal proportions, and calcium carbonate is predominantly intact charophyte encrustations rather than fine-grained calcite. Sediments accumulating below the thermocline (≥7 m) contain significantly more organic matter (>60%) than calcium carbonate (<20%). This relationship appears to be related to acidity, temperature and dissolved oxygen in the water column (e.g., Stabel, 1986; Dean and Megard, 1993; Dean 1999; Ramisch *et al.*, 1999). At depositional locations below the thermocline, raining carbonate particles apparently dissolve, either during deposition or before burial. Raining carbonate particles accumulate at depositional sites located above the thermocline.

In our interpretation we assume the following sedimentation scenarios. If water depths were ≥5 m (within or below the thermocline) at a given depositional location, then organic matter accumulation would exceed that of calcium carbonate. This occurs because carbonate is dissolved either within the thermocline, in the hypolimnion or at the sediment–water interface. In contrast, if water depths were ≤5 m (above the thermocline) then calcium carbonate accumulation would increase relative to organic matter. Furthermore, in littoral zones, lower water levels could create sedimentary unconformities by wave action, thereby decreasing shallow-water sedimentation rates. In contrast, deep-basin sedimentation rates would be uninterrupted and rapid as a result of sediment focusing. The possibility also exists that sediment re-working

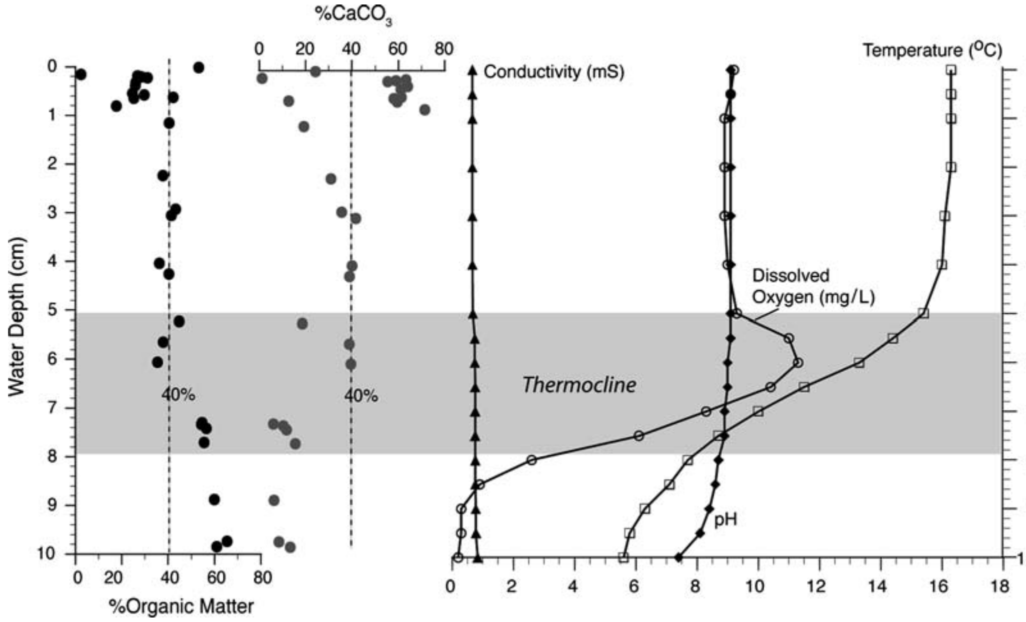

Figure 2 Surface sediment %LOI (unpublished data, 2004, courtesy of L.C. Cwynar) and water column measurements of Marcella Lake in July 2000

because of lower water levels could disrupt sedimentation, resulting in displaced material at depth.

Methods

Bathymetry was determined by fish-finder soundings. A Hydrolab Surveyor 4 and Datasonde 4 were used to collect water column temperature, pH, specific conductivity and dissolved oxygen. Sediment cores were retrieved from a platform with a modified square rod piston corer at 1.95, 4.30, 6.97 and 9.60 m below modern level (BML) (Figure 1). Sediments were visually logged for Munsell colour, sedimentary structures, biogenic features and smear-slide features. Magnetic susceptibility was measured on half cores at 5-mm intervals with a Bartington Susceptibility Meter. Smear-slide analyses showed that mineral-rich sediments (lower organic and carbonate content) were higher in dry bulk density and higher in magnetic susceptibility. Organic matter (% organic matter) and calcium carbonate content were determined by the loss-on-ignition (%LOI) method (Bengtsson and Enell, 1986; Heiri *et al.*, 2001). Weight% $CaCO_3$ was based on the following calculation of the mass lost after a 4-h burn at 1000°C: [%$LOI_{1000°C}$*(100/44)]. Elemental carbon (% organic carbon) and nitrogen content and $\delta^{13}C$ and $\delta^{15}N$ were analysed on selected samples after acid pretreatment using an elemental analyser coupled with a Finnigan Delta-plus mass spectrometer. Isotope sample reproducibility is ±0.2‰. Carbon and nitrogen isotope ratios are reported in δ-notation, $\delta = ([R_{sample}/R_{standard}] - 1) \times 1000$ where $R = {}^{13}C/{}^{12}C$ or ${}^{15}N/{}^{14}N$, and are expressed as per mil (‰) relative to the international standards: Vienna Peedee Belmnite (VPDB) for carbon and air (VAIR) for nitrogen.

The core chronologies are based on AMS radiocarbon dates from terrestrial macrofossils (Table 1) and the median calibrated (2-sigma) age of the White River tephra, 1150 cal. BP (Clague *et al.*, 1995). At stratigraphic levels where terrestrial macrofossils were not present in sufficient quantities, intact aquatic macrofossils and purified spruce pollen samples were used (Brown *et al.*, 1989). Radiocarbon ages were calibrated using CALIB 4.0 following the methods of Stuiver *et al.* (1998). Both the measured radiocarbon and median calibrated ages are reported but only calibrated ages are used for discussion. Rates of sedimentation were determined by linear interpolation between dated stratigraphic depths.

Results

The cores were taken on a transect from deep to shallow water (Figure 1). Core A and B were taken within 2 m of each other at 960 cm BML and have overlapping stratigraphic intervals. The cores were matched visually and with bulk sediment data to make composite core A/B (Figures 3 and 4). Core F was taken on the slope between A/B and C/E. It contained 340 cm of reworked lacustrine mud interspersed with shell lag deposits. With the exception of an AMS radiocarbon age of the basal sediments, no other sedimentary analyses were performed on core F. Core C and E were taken within 1 m of each other at 430 cm BML. They contain overlapping stratigraphic intervals and were matched in a similar manner as A and B (Figure 5). Core D (195 cm BML) contained 360 cm of stratigraphically intact sediment (Figure 6). Sedimentary facies descriptions and water depth interpretations are summarized in Table 2.

Core A/B (960 cm BML)

Bulk sedimentary data and the pollen record from core A/B contain features that indicate a sedimentary discontinuity, both when examined for internal consistency and compared with Cwynar's (1988) record. At 428.5 cm depth, bulk sedimentary values are abruptly interrupted and a visible centimetre-scale unconformable surface occurs. The overlying dark brown organic-rich sediments upwards to ~260 cm depth contain disturbed textures, and otherwise rare aquatic mosses, and produced suspiciously old radiocarbon ages (Table 1). Figure 3a shows percentages of key pollen taxa with depth for the whole section, prior to any adjustments. Upwards from near the base, the early spruce zone (~470–425 cm) shows increasing *Picea*, stable *Juniperus* and *Alnus*, and decreasing *Betula*, *Salix*, *Populus*, *Artemisia* and *Cyperaceae*. Between the samples at 428.5 cm and 408.5 cm these patterns are abruptly interrupted and succeeded by a zone (labelled 'displaced material') in which taxa prominent prior to the spruce rise dominate, and *Picea* and *Juniperus* are largely absent. Towards the top of this zone (~340–300 cm), small quantities of *Picea* and *Juniperus* reappear, suggesting that there may have been some mixing of the sediments as the displaced material moved. From ~300–260 cm, the pollen curves are almost identical to those of the early spruce zone and this repeat is taken to mark the uppermost portion of the displaced material. Figure 3b shows that removal of the suspect material (thickness, according to the pollen stratigraphy, ≤170 cm) yields a pollen curve consistent with Cwynar's (1988). Statistically identical radiocarbon ages from depths immediately above (259 cm) and below (429 cm) provided further constraints on the thickness of the displaced material and the timing of the event (~7850 cal. BP). Figure 4 shows core A/B stratigraphy and bulk sedimentary data after removing the suspect sediment (unit 3a) and adjusting the depths for samples below 260 cm.

Overlying basal gravel (unit 4), unit 3c (348–328 cm, corrected depth) is composed of grey, silty marl characterized by a relatively high magnetic susceptibility (>3 SI), high dry bulk density (>0.6 g/cm^3), low organic carbon (<30%; elemental analyser method) and high calcium carbonate (>40%) primarily in the form of bivalve shell fragments. $\delta^{13}C$ values are low (−31‰) and C/N ratios are relatively low (12). A radiocarbon age reversal indicated on an aquatic macrophyte at 505 cm, 10 650±50 (OS-12130), indicates either a significant reservoir effect or sediment re-working.

The lower boundary of unit 3b (328–260 cm, corrected depth) is marked by a transition to strongly laminated organic marl. The shift is distinguished by decreased magnetic susceptibility (0 SI), decreasing dry bulk density (<0.2 g/cm), increased organic carbon (30–40%) and highly variable but lower carbonate content (20–40%). C/N ratios rise to ~14 and $\delta^{13}C$ values increase (−28‰). Radiocarbon ages of 8605±40 (CAMS-96834) and 8560±60 (OS-12129), at 296 and 288 cm corrected depths, respectively, and 7060±40 (CAMS-73154) at 259 cm corrected depth, support the stratigraphic integrity of unit 3b.

Lowermost unit 2b (260–165 cm) is dark-brown organic mud, which becomes olive-brown faintly laminated organic mud up-core. Organic carbon, calcium carbonate and C/N ratios increase while $\delta^{13}C$ remains relatively unchanged. Unit 2a (165–90 cm) is marked by a transition to black, gelatinous organic mud containing micro-scale laminae. Smear-slide analyses indicated the laminae alternate between diatoms and fine-grained organic mud. Both organic carbon and calcium carbonate decrease, presumably because of an increased proportion of biogenic silica in the diatom laminae.

Table 1 AMS Radiocarbon data from Marcella Lake

Core name	Core depth (cm)	Depth BML (cm)	Material	Lab. no.	Measured age (^{14}C-yr BP)	Median calibrated age (cal. BP)	1 sigma range
Marcella Core A	31	991	Charcoal	CAMS-96830	1085±35	970	952–1051
Marcella Core A	101	1061	Wood	CAMS-96832	2365±40	2350	2345–2358
Marcella Core B	181	1141	Wood	CAMS-73153	4520±40	5140	5050–5301
Marcella Core A	198	1158	Wood	CAMS-73144	5330±40	6070	5995–6181
Marcella Core A	241	1201	Wood	CAMS-73145	7370±110	8180	8031–8333
Marcella Core B	259	1219	Wood	CAMS-73148	7000±40	7800	7757–7922
Marcella Core A	*328.5*	*1288.5*	*Seed+wood*	*CAMS-98814*	*8955±55*	*10170*	*9923–10210*
Marcella Core A	*361*	*1321*	*Macros+seeds*	*CAMS-96833*	*9260±40*	*10445*	*10289–10500*
Marcella Core A	*378.5*	*1338.5*	*Aquatic macro*[a]	*CAMS-73146*	*11110±50*	*13135*	*12990–13171*
Marcella Core B	*405*	*1365*	*Wood*	*CAMS-73147*	*9200±50*	*10330*	*10241–10474*
Marcella Core A	429	1389	Wood	CAMS-73154	7060±40	7900	7793–7938
Marcella Core B	458	1418	Wood	OS-12129	8560±60	9530	9499–9550
Marcella Core A	466	1426	Wood	CAMS-96834	8605±40	9550	9533–9553
Marcella Core B	478	1438	Aquatic macro[a]	OS-12130	10650±50	12715[a]	12631–12894
Marcella Core A	520	1480	Wood	OS-12131	9090±55	10220	10213–10242
Marcella Core E	41	471	Wood	OS-38713	930±25	830	791–915
Marcella Core C	44	474	Plant stem	CAMS-96826	980±60	925	793–951
Marcella Core E	133	573	Wood	OS-38714	4080±35	4545	4451–4781
Marcella Core C	154	584	Wood	CAMS-96827	3880±90	4330	4152–4420
Marcella Core C	161	591	Aquatic macro[a]	CAMS-73149	4410±50	5020[a]	4870–5047
Marcella Core C	174	604	Wood	CAMS-96828	4980±40	5665	5655–5743
Marcella Core D	233	428	Aquatic macro[a]	CAMS-73150	3830±60	4200[a]	4098–4350
Marcella Core D	327.5	522.5	Wood	CAMS-96829	7770±110	8580	8413–8638
Marcella Core D	353	548	Seed	CAMS-73151	8530±130	9530	9433–9595
Marcella Core D	359	554	Seed	CAMS-73152	8840±120	10100	9634–10177
Marcella Core F	337	1037	Pollen[b]	CAMS-92157	6595±40	7475[b]	7430–7561

[a]Aquatic material is suspect because of possible hard water effects.
[b]Brown *et al*. (1989).
Ages in italic are within the displaced material removed from the adjusted A/B stratigraphy (Figure 4).
Depths in parentheses are corrected for displaced material removed from the adjusted stratigraphy (Figure 4).

δ^{13}C increases (−26‰), C/N ratios decrease and δ^{15}N decreases by 4‰.

The transition from unit 2a to unit 1 at 95 cm is a gradual change in colour and texture. Unit 1 is faintly colour banded, bioturbated, olive-brown, gelatinous, organic mud. The 1.0 cm thick White River tephra (Clague *et al*., 1995) occurs at 64 cm. Organic carbon is lower than in unit 2a (35–40%) and calcium carbonate content is higher (15–25%), δ^{13}C decreases and C/N ratios are relatively unchanged. Radiocarbon ages are in stratigraphic order after adjusting for the displaced material (Table 1) except for a reversal between 241 and 249 cm. A linear age model (after adjustment) indicates faster sedimentation rates between 10 000 and 8000 cal. BP and slower rates since 8000 cal. BP (Figure 4).

Core F (697 cm BML)

With the exception of the lowermost portion of the section, core F is composed of chaotically structured dark-brown organic mud interspersed with shell lag deposits and bryophyte layers. The White River tephra was neither visible nor detected by magnetic susceptibility. However, overlying basal gravel is faintly laminated marl. Spruce pollen was extracted 3 cm above the base of the core within this laminated sediment. The resultant age 6595±40 (CAMS-92157; 7477 cal. BP; Table 1) was used to identify the approximate onset of lacustrine sedimentation at this location.

Core C/E (430 cm BML)

Overlying basal gravel, unit 4 (200–185 cm) is grey-brown, silty, organic mud containing abundant mollusc shell fragments. Magnetic susceptibility and dry bulk density are low (0 SI, 0.2–0.3 g/cm^3). Organic matter (%LOI method) is between 20 and 25% and calcium carbonate fluctuates between 60 and 70%. The transition to unit 3 is a gradual colour and textural change.

Unit 3 (185–155 cm) is brown, bryophyte-rich, organic mud containing mollusc shell fragments and *Chara* encrustations. At the base of unit 3, macrophyte fragments interrupt bands of mollusc shells on an unconformable surface (177 cm). Magnetic susceptibility peaks, organic matter increases and calcium carbonate decreases. The upper portion of unit 3 is macrophyte-rich organic mud. Another unconformable surface marks the boundary between unit 3 and unit 2, where there is a rise in magnetic susceptibility, increased organic matter and decreased calcium carbonate.

Unit 2 (155–130 cm) is olive-brown, strongly laminated, fine-grained, organic marl containing abundant and well-preserved *Chara* encrustations. Magnetic susceptibility and dry bulk density are low (0 SI, 0.3–0.4 g/cm^3). Organic matter is between 20 and 30% while calcium carbonate is between 40 and 60%. The transition to unit 1 is a gradual shift towards lower organic matter content and higher calcium carbonate content. Unit 1 (130–0 cm) is light, olive-brown, fine-grained, strongly laminated marl containing abundant well-preserved *Chara* encrustations. The White River tephra is 1.0 cm thick at 64 cm depth. Radiocarbon ages and the White River tephra are in stratigraphic order (Table 1). A linear age model suggests slower sedimentation rates between ~5500 and 4000 cal. BP and more rapid rates to the present (Figure 5).

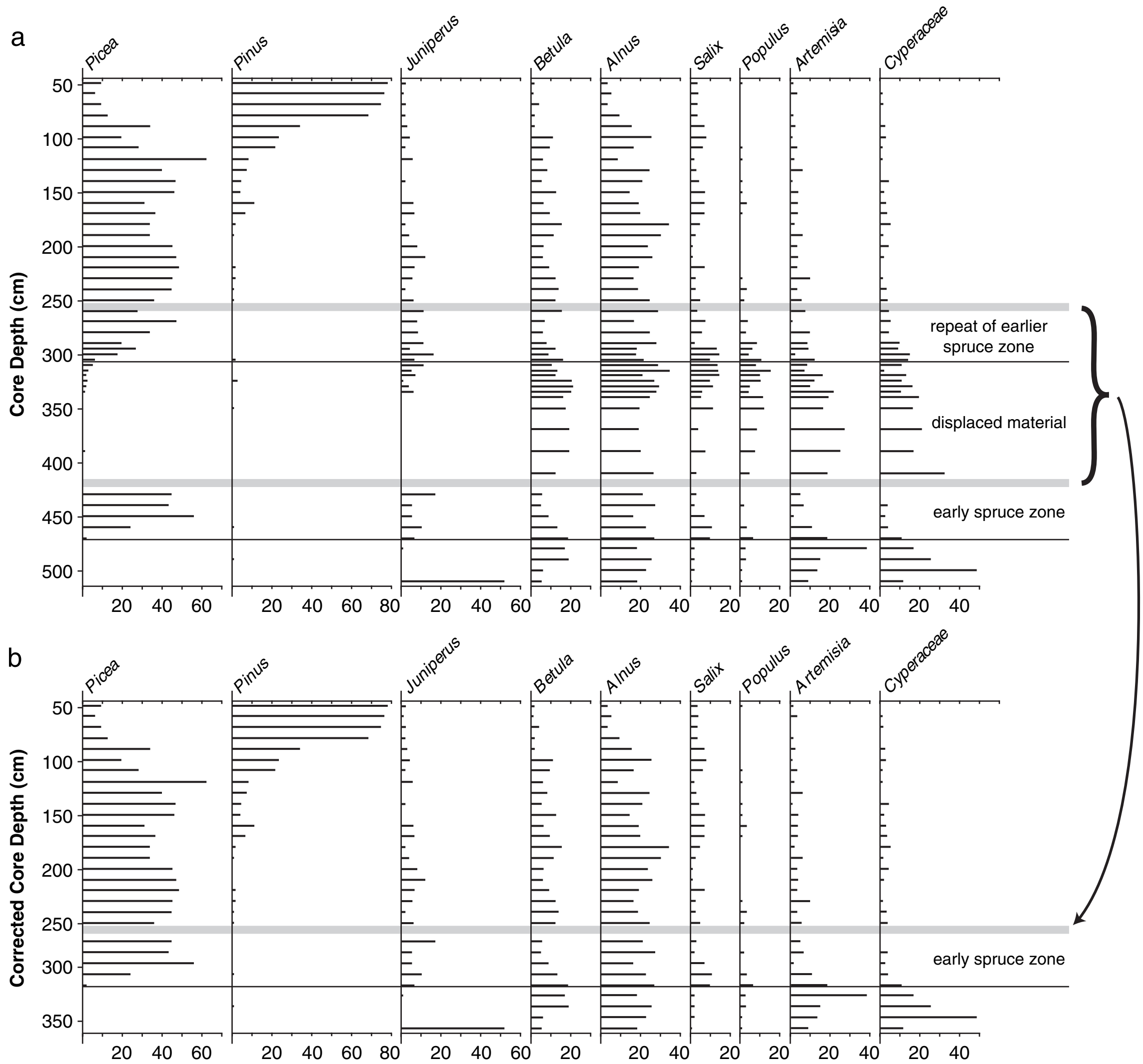

Figure 3 Core A/B pollen percentages of key taxa with depth for: (a) the whole section without adjustment and (b) after adjustment by removing suspect material between 429 and 260 cm depth.

Core D (195 cm BML)

Core D was taken near the submerged *Chara* vegetation in the southeast bay (Figure 1). Living *Chara* varied in thickness between 30 and 50 cm and the coring site was chosen to avoid penetrating living vegetation. Overlying basal gravel, unit 3 (360–330 cm) is dark olive-brown, strongly laminated organic mud containing mollusc and gastropod shell fragments. Magnetic susceptibility and dry bulk density are low (0 SI,

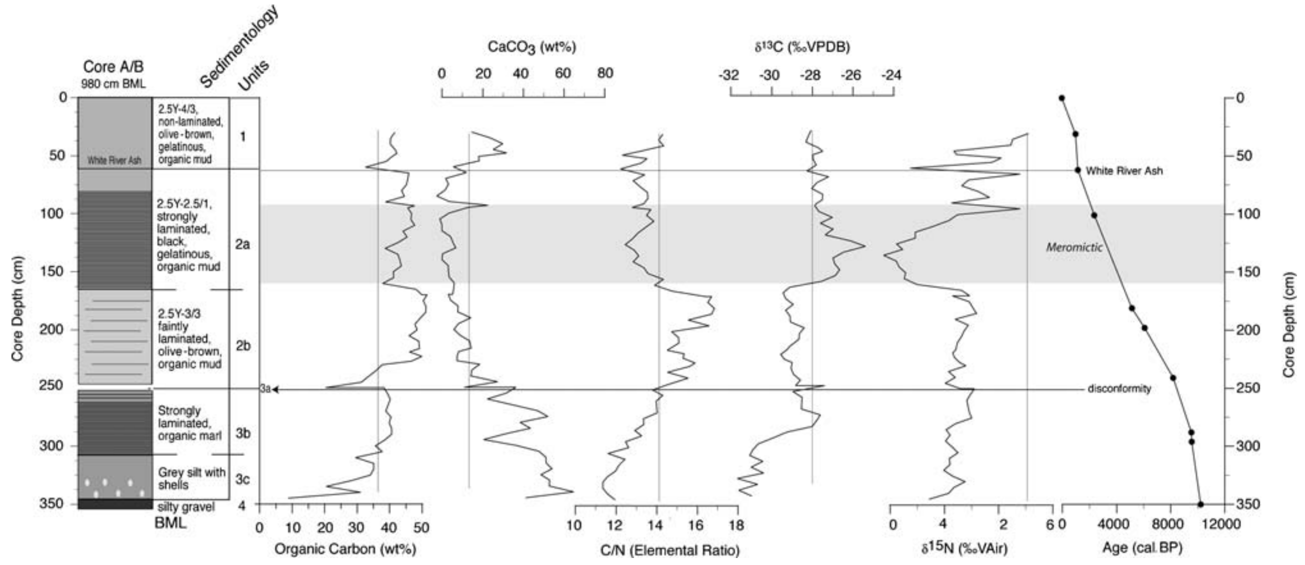

Figure 4 Core A/B, 960 cm water depth, showing stratigraphy, organic carbon (elemental analyser method), calcium carbonate, C/N, $\delta^{13}C$, $\delta^{15}N$ and median calibrated radiocarbon ages by depth

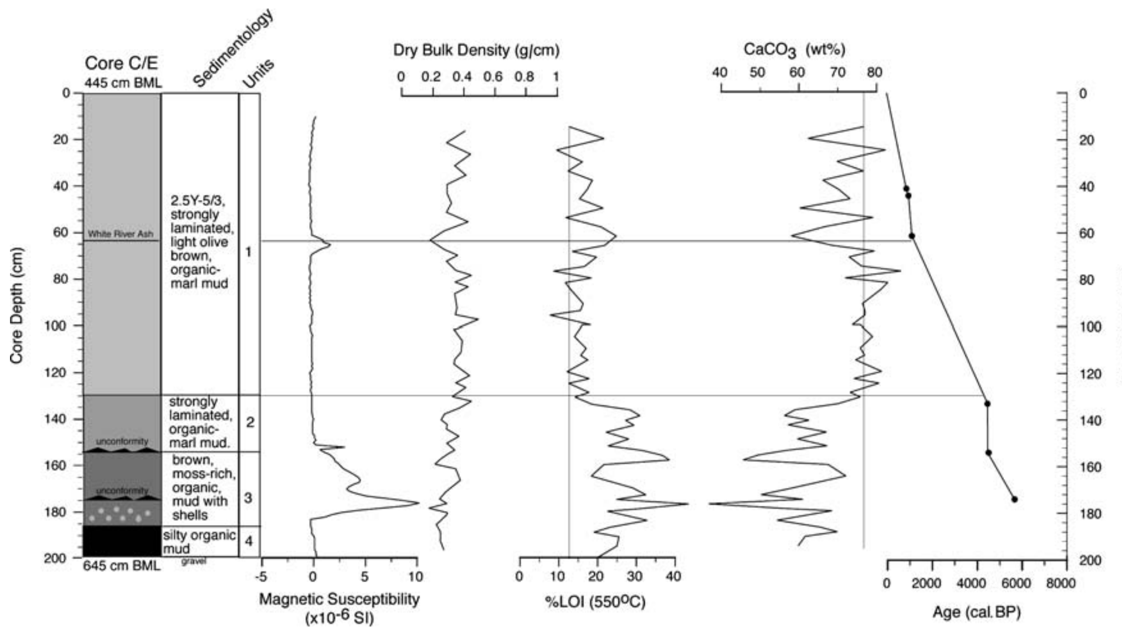

Figure 5 Core C/E, 430 cm water depth, showing stratigraphy, magnetic susceptibility, dry bulk density, organic matter (%LOI method), calcium carbonate and median calibrated radiocarbon ages by depth

0.2–0.4 g/cm^3), organic matter (%LOI method) varies between 20 and 30% and calcium carbonate (%LOI method) varies between 60 and 80%.

Strongly laminated structures are disrupted at the boundary between unit 3 and unit 2 (330–245 cm). At the base of unit 2 there are bands of mollusc shell fragments overlain by disturbed, fine-grained, organic mud. Variability of organic matter and calcium carbonate content increases in unit 2. Four or possibly six unconformable surfaces were visually identified.

The transition from unit 2 to unit 1 (245–0 cm) is identified by a change to strongly laminated, light olive-brown, fine-grained, organic marl containing abundant *Chara* encrustations. Dry bulk density increases, organic matter decreases and calcium carbonate increases. Based on cores A/B and C/E, the depth of the White River tephra would be 58 to 66 cm depth, but the tephra was not visible or magnetically detected. Instead, a band of green, unusually well-preserved *Chara* vegetation occurs at 68 cm. Between 40 and 70 cm, increased dry density, decreased organic matter and increased calcium carbonate may indicate an unconformity or re-working. Radiocarbon ages in core D are in stratigraphic order (Table 1). Similar to core C/E, sedimentation rates prior to 4200 cal. BP were slower. The radiocarbon age at 233 cm of 3830 ± 60 (CAMS-73150) could be too old because of hard water effects but if the age is accurate, then after 4200 cal. BP core D rates are higher than core C/E. At the core D site, sediments appear to have accumulated on a flat shelf, while core C/E sediments dip 15° towards the deep basin, possibly leading to some down-slope sediment sloughing.

Discussion

If our lake-level thermocline model is correct we can use sedimentary properties to infer past water depth. When water depths were ≤ 5 m in the deep basin, there was an unstratified

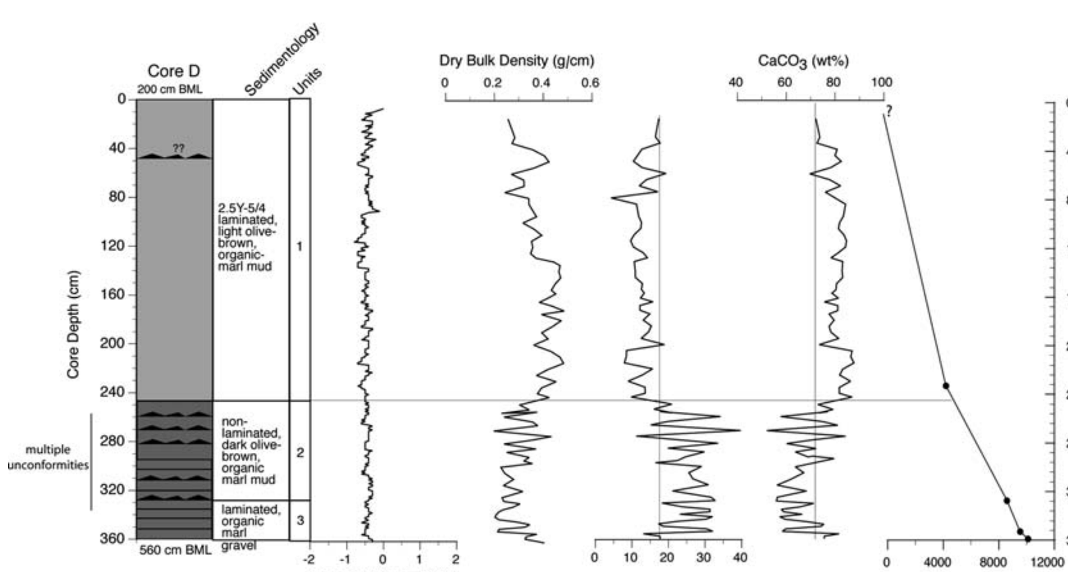

Figure 6 Core D, 195 cm water depth, showing stratigraphy, magnetic susceptibility, dry bulk density, organic matter (%LOI method), calcium carbonate and median radiocarbon calibrated ages by depth

Table 2 Sediment description and lake-level interpretation with estimated ages

Core	Unit	Description	Interpretation	Est. age (cal. BP)
A/B	1	Olive-brown gelatinous organic mud Irregular, faint laminations	Modern depth, ~9.7 m	2–0
	2a	Black gelatinous organic mud Millimetre-scale diatom laminations	> 10 m water depth. Meromixis	4.5–2.0
	2b	Dark olive-brown organic mud Faint colour banded structure	6–8 m water depth	7.5–4.5
	3a	Dark-brown organic mud Unconformity at base of unit	Displaced sediment. Possible low-stand	8.0–7.5
	3b	Strongly laminated brown organic marl Shells. Unconformity at base	9–10 m water depth	9.5–8.0
	3c	Dark grey silty marl	Re-worked shoreline sediment Rising lake-levels	10.0–9.5
	4	Gravel and sand	Subaerial exposure	> 10
C/E	1	Light olive-brown strongly laminated organic marl Well-preserved *Chara*	4–6 m water depth	4.5–0
	2	Olive-brown, strongly laminated organic marl Poorly-preserved *Chara*. Unconformity at base	> 6 m water depth	5.0–4.5
	3	Dark brown macrophyte-rich organic mud Strongly laminated. Poorly preserved *Chara* Bivalve shells	1–3 m water depth	6–5
	4	Grey-brown shelly silt	Reworked shoreline sediment	7.5–6.0
D	1	Light olive-brown strongly laminated organic marl. Well-preserved *Chara*	3–5 m water depth	4.5–0
	2	Olive-brown organic marl. Shells Multiple unconformities	Reworked shoreline sediment	8.5–4.5
	3	Dark olive-brown strongly laminated organic mud. Bivalve shells	1–2 m water depth	10.0–8.5
		Gravel	Subaerial exposure	> 10

water column and calcium carbonate accumulation exceeded that of organic matter. Following this model, down-core sedimentary properties interpreted as low lake-level facies include: (i) colour banded or laminated fine-grained micrite containing plant macrophytes, ostracode tests and *Chara* crusts, (ii) mollusc shell-lags and (iii) abrupt sedimentary unconformities (see Table 3, a classification of magnetic susceptibility, dry density, organic matter or organic carbon, calcium carbonate, δ^{13}C, C/N and δ^{15}N ratios). In contrast, water depths ≥ 8 m are associated with a thermally stratified water column and permanent or temporary meromictic conditions. Sedimentary properties interpreted as deep-water facies include strongly laminated dark-brown or black gelatinous organic mud with bulk sedimentary characteristics that are distinct from those of shallow water facies (Table 3). For example, in core A/B unit 2, when laminations indicate the lake was meromictic, organic matter δ^{13}C ratios were high, C/N ratios were relatively low and δ^{15}N ratios were very low (Figure 4). Meromictic conditions may be caused by a number of factors including higher lake level, shifts in biological productivity resulting from increased nutrient loading by watershed run-off, or longer ice cover duration causing diminished spring and autumn overturn. Either of the first two possibilities supports an increase in the regional effective moisture and the third case, ice cover, is an unlikely explanation.

Mixing regime variations may be a significant factor for carbon and nitrogen isotope variations (e.g., Hodell *et al.*, 1998). Organic matter δ^{13}C records the isotopic composition of lake-water dissolved inorganic carbon (DIC). DIC is in turn a reflection of organic carbon sequestration rates and carbon isotope ratios of CO_2 sources from atmospheric dissolution, biological respiration and groundwater (Oana and Deevey, 1960; McKenzie, 1985; Dean and Stuiver, 1993). It has been observed that during thermal stratification, DIC pools within the epilimnion and hypolimnion evolve in isolation. In the epilimnion, sequestration of ^{12}C-enriched DIC into organic matter eventually leads to the accumulation of ^{13}C-enriched DIC and progressively higher organic matter δ^{13}C values. In contrast, hypolimnion DIC becomes relatively ^{13}C-depleted because the primary DIC source is respired ^{12}C-enriched CO_2. Mixing epilimnion and hypolimnion DIC pools tends to decrease epilimnion-DIC δ^{13}C values and hence organic-matter δ^{13}C values (Hodell *et al.*, 1998). Organic matter δ^{15}N is possibly related to the degree of nitrogen recycling within the lake (Kendal, 1998).

Lake-level reconstruction

Figure 7 shows the lake-level reconstruction; stratigraphic data are shown as depth below modern level (BML) on a calibrated age scale. Radiocarbon ages illustrate relative sedimentation rates at each site and sedimentary interpretations (Table 2) provide maximum and minimum water-depth estimates indicated by the grey shading. The thickness of the grey shading indicates the range of water-depth estimates.

The lowermost sediment in A/B and D suggest lake level initially rose 9 m (4 to 5 m BML) soon after deglaciation. Intact sediment from the southeastern slope appears to have been displaced into the deep basin ~8000 cal. BP (unit 3a core A/B). This resulted in an apparent delay in the onset of sedimentation at F (7500 cal. BP) and slow, disturbed sedimentation at D (unit 2). Such slope failures are due to instability that could be caused by a variety of events including seismic activity, sediment de-gassing or lower lake levels that expose shelf sediments to wave action. If the slope failure was due to a lower lake stand, water levels could have lowered 3 m (7–8 m BML). After 7500 cal. BP, deep-water sedimentation at A/B (unit 2b) and shallow sedimentation at C/E (unit 3)

Table 3 Summary of bulk sediment properties and inferred water depth

Measurement	> 8 m deep	5–8 m deep	< 5 m deep
Magnetic susceptibility	0 (SI)	0 (SI)	0–10 (SI)
Bulk density	0.1–0.2 (g/cm)	0.1–0.2 (g/cm)	0.3–0.5 (g/cm)
% LOI (55°C)	60–80%[a]	30–40%	10–20%
% $CaCO_3$	0–20%	30–40%	70–80%
$\delta^{13}C$	−26 to −27.5‰	−28.5 to −29.5‰	−30.5 to −31.5‰
$\delta^{15}N$	0 to −1‰	2–3‰	2–3‰
C/N ratio	14.0–16.5	11–13	12–13

[a]%LOI (550°C) values are ~2.8× larger than %organic carbon for comparison with core A/B values in Figure 4.

suggest lake level was 4 m BML. It likely remained stable until 5000 cal. BP, when several lines of evidence suggest an additional lake-level lowering by 1.5–2 m. These include an unconformity at 600 cm BML at C/E (unit 2), multiple unconformities between 550 and 460 cm BML at D (unit 2) and water depths between 5 and 7 m BML at A/B (unit 2b). The lake was meromictic probably resulting from a higher lake level between 4000 and 2000 cal. BP. In addition to the diatom laminae at A/B (unit 2a), rising water levels are indicated at C/E (unit 2 and 1) and by water depths from 2.5 to 5 m at D (unit 1). Indications of raised shorelines are circumstantial evidence in support of this hypothesis, but require further investigation (L.C. Cwynar, personal communication, 2005). A possible unconformity between 258 and 266 cm BML in D (unit 1), and increasing calcium carbonate in A/B (unit 1) support subsequently lower lake levels since 2000 cal. BP.

Holocene palaeoclimate

The lake-level reconstruction indicates that, after correcting for sediment infilling, water levels were 3 m lower than modern

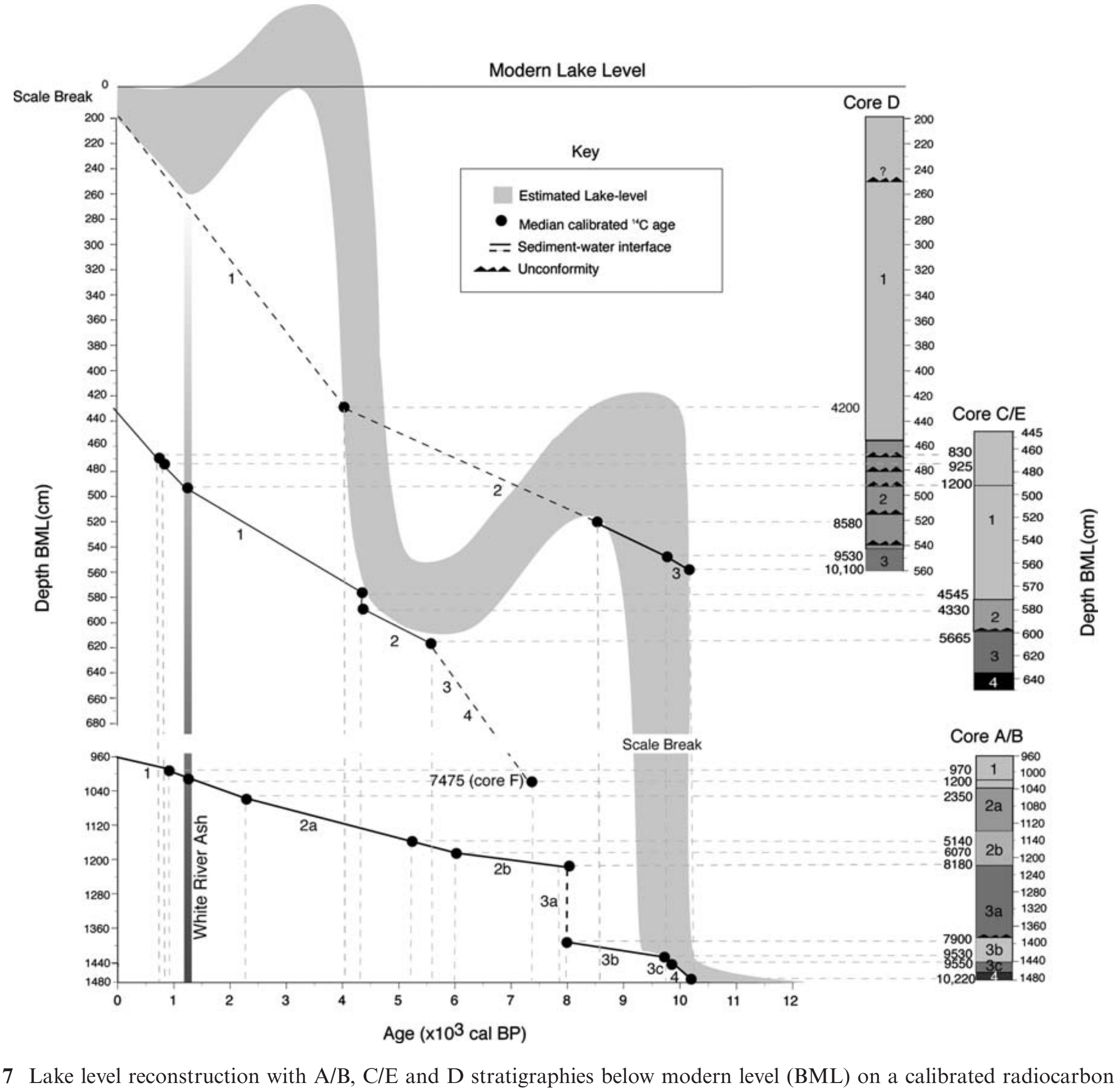

Figure 7 Lake level reconstruction with A/B, C/E and D stratigraphies below modern level (BML) on a calibrated radiocarbon age scale. Lines between calibrated ages (solid circles) indicate continuous sedimentation (solid line) and discontinuous sedimentation (dash). Grey shading represents lake-level estimates

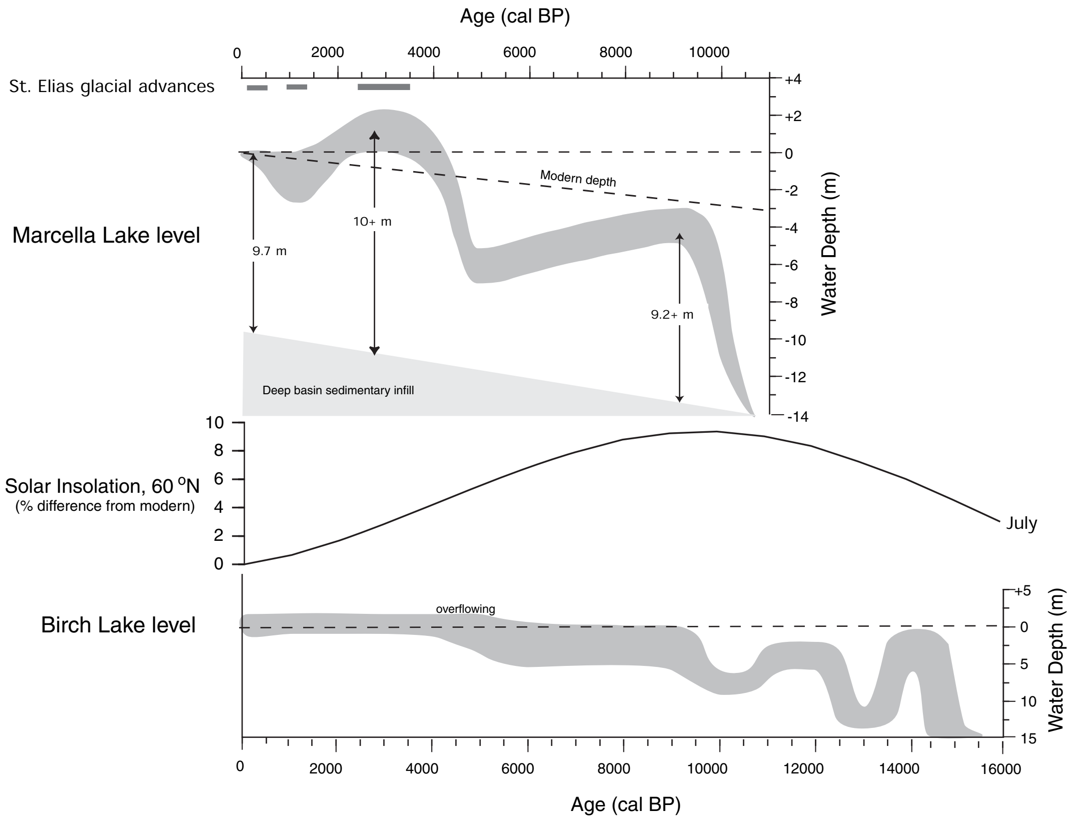

Figure 8 Correlation on a calibrated radiocarbon timescale of Marcella Lake water levels with glacier activity in the St Elias Mountains (Denton and Karlén, 1977), July insolation at 60°N (Berger and Loutre, 1991) and water levels at Birch Lake, Alaska (Abbott *et al*., 2000). High stands occurred when summer insolation was high in early Holocene and when it was relatively low in the late Holocene

between 10 000 and 5000 cal. BP, higher than modern between 4000 and 2000 cal. BP and slightly below or near modern after 2000 cal. BP (Figure 8). This lake-level history corresponds with the climatic history inferred from pollen by Cwynar's (1988) core retrieved at 760 cm BML (Figure 1) and is reflected in the pollen record (Figure 3b). Cwynar (1988) used an age model derived from 15 conventional radiocarbon dates of bulk sediment. Although there is some difference in timing (probably related to the different properties of bulk sediment dates) the two records are broadly consistent. The abundance of *Populus* (poplar) and *Artemisia* (sage) prior to 10 000 cal. BP is interpreted as evidence of a warm, dry climate. Rising water levels after 10 000 cal. BP correspond with the appearance of *Picea glauca* (white spruce), suggesting increasing effective moisture. By 6000 ^{14}C BP (6800 cal. BP), the *Picea glauca* (white spruce) woodland changed to a mixed spruce forest dominated by *Picea mariana* (black spruce), possibly indicating an increase in effective moisture (Cwynar, 1988; see also Cwynar and Spear, 1995). Rising lake levels also indicate increasing effective moisture, but only after 4000. cal. BP. An overall decline in spruce and the disappearance of *Picea mariana* by 2000 ^{14}C BP (2000 cal. BP) corresponds with the establishment of lodgepole pine (*Pinus contorta*). It is unclear if this shift was driven by climate. Its timing at Marcella Lake coincides with decreasing lake levels. A comparison of these results with other regional proxies for early, middle and late Holocene palaeoclimate follows.

Early Holocene (11 000–7500 cal. BP)

During glacial times, lower sea level in addition to cooler North Pacific sea surface temperatures reduced moisture advection to interior regions (Mann and Hamilton, 1995). Pollen studies in Alaska and terrestrial evidence in the Yukon reflect late glacial aridity (Wang and Geurts, 1991; Bigelow and Edwards, 2001; Lauriol *et al*., 2001, 2002). Rising sea level correlates with initial lake-level rises in Birch Lake (Abbott *et al*., 2000). The climatic response in the southwest Yukon to rising late-Pleistocene sea levels was delayed, perhaps by local climatic effects caused by the Cordilleran ice sheet. The first wet phase in Marcella Lake occurred later, between 10 000 and 9000 cal. BP, which appears to correlate with the third wet phase at Birch Lake.

Several environmental changes in the northern Yukon indicate climate was warmer during this period when solar insolation was at a maximum. Spruce micro- and macrofossils found on the north coast suggest a northward position of boreal forest tree line (Ritchie *et al*., 1983). Additionally, a prevalent thaw unconformity dating ~9000 cal. BP formed at the base of an active layer 2.5 times thicker than present (Burn, 1997). In the central Yukon, a thaw unconformity dates ~9500 cal. BP (Burn *et al*., 1986). Northern Yukon thaw lake formation was at a maximum ~9000 to 8000 cal. BP (Mackay, 1992). In the southern Yukon, the early part of this period was arid, compared with the present day or the middle Holocene. These data are evidence for a warm and dry early Holocene. At 9000–10 000 cal. BP there was a rapid increase in lake level, suggesting a shift in the precipitation regime. The early aridity may have prevented the regional establishment of spruce forest.

Middle Holocene (7500–4000 cal. BP)

Between 7500 and 5000 cal. BP lake levels were relatively stable 5 m BML, indicating conditions considerably drier than present and the immediately preceding period. This is consistent with reduced snow accumulation in the alpine zone of the southwest Yukon between 6700 and 4700 ^{14}C-yr BP (Farnell *et al*., 2004), but conflicts with a high-resolution diatom-inferred salinity profile in the central Yukon that indicates a wet middle Holocene (Pienitz *et al*., 2000). In terms of temperature, fossil spruce deposits on the eastern slopes of the St Elias Mountains were found up to 70 m higher than modern tree line, suggesting warmer conditions at 6500 cal. BP (Denton and Karlén, 1977). Later, temperatures in the northern Yukon decreased. Peat-land permafrost development by 4700 cal. BP suggests decreasing temperatures (Vardy *et al*., 1997) and ice-wedge growth, which was uncommon in the early Holocene, was underway by 4500 cal. BP (Mackay, 1992).

Late Holocene (4000 cal. BP to present)

Regional cooling occurred during a period of higher than modern water levels between 4000 and 2000 cal. BP and is contemporaneous with valley glacier advances in the St Elias Mountains (Denton and Karlén, 1977). Three intervals of glacier expansion were documented (3400–2400, ~1200 and 400–90 cal. BP) (Figure 8). Thus, as in central and northern Alaska, late Holocene glacial advances in the southwest Yukon appear to coincide with increasingly wet climatic conditions in addition to a millennial-scale decrease in summer insolation (Anderson *et al*., 2001; Lamoreux and Cockburn, 2005). Fossil spruce found above modern tree line dated between 4000–3000 and 2000–1000 cal. BP, suggest favourable growing conditions occurred at times during a generally cooler and moister late Holocene. Marcella Lake levels dropped to near or slightly below modern by 2000 cal. BP. This shift corresponds with increases in the palaeosalinity documented by Pienitz *et al.* (2000) that also suggest increasing aridity. The resolution of the lake-level estimates is limited, but continuous sedimentation at shallow depths indicates water levels have remained near modern, with no major lowering since 1200 cal. BP. Recent glacial advances since 400 cal. BP represent, in most cases, maximum advances since deglaciation (Calkin *et al*., 2001) and probably reflect significant cooling during the 'Little Ice Age'. Thus, the late Holocene has trended away from a moisture maximum and conditions during the last millennium have likely been drier than any since the middle Holocene.

Conclusions

Holocene sedimentation at Marcella Lake can be interpreted in terms of lake-level variation, providing a quantitative record of effective moisture variability. An early Holocene lake-level rise may have been significant for the regional establishment of spruce forest, but the region remained drier than present until 4000 cal. BP. Early Holocene high stands in Marcella Lake coincide with higher than modern summer insolation. Wetter than modern conditions probably occurred between 4000 and 2000 cal. BP, and coincide with the onset of late Holocene glacial activity and decreasing summer insolation. Nevertheless, after 2000 cal. BP lake levels dropped and Little Ice Age glacial advances occurred under drier conditions than preceding millennia.

This long-term moisture record, together with modern climatological observations, allows us to propose a hypothesis for circulation adjustments that have controlled Holocene moisture changes. Moisture delivery in the region is strongly influenced by the strength and position of the Aleutian Low centred over the Gulf of Alaska. A weakened Aleutian Low favours more zonal atmospheric flow that could allow more moisture to reach interior areas. Such a scenario could be invoked for the period between 4000 and 2000 cal. BP when lake levels were higher than today. In contrast, when effective moisture trends reversed 2000 cal. BP, the Aleutian Low may have intensified, enhancing meridional on-shore airflow that intensifies the rain shadow effect and restricts moisture flow to the interior. Indeed, an increasing body of evidence suggests just such a mechanism (Spooner *et al*., 2003; Anderson *et al*., 2005) and forthcoming research will evaluate this hypothesis in further detail (e.g., Fisher *et al*., 2004). This lake-level reconstruction serves to constrain the timing and direction of large-scale changes in effective moisture and thereby provide a framework for further, more detailed studies.

Acknowledgements

The authors wish to thank Les Cwynar for contributing surface sediment data and his insights to this study. Joseph Rodgers and Britt Haugen assisted in the field and Andrea Krumhardt, Trent Hayden, and Bronwen Whitney in the lab. Two anonymous reviewers provided helpful comments that improved the mansucript. This research was supported by grants from the National Science Foundation (ATM-0296157 and ATM-0097127) and the Department of Geosciences at the University of Massachusetts Amherst.

References

Abbott, M.B., Finney, B.P., Edwards, M.E. and **Kelts, K.R.** 2000: Lake-level reconstructions and paleohydrology of Birch Lake, Central Alaska, based on seismic reflection profiles and core transects. *Quaternary Research* 53, 154–66.

Anderson, L., Abbott, M.B. and **Finney, B.P.** 2001: Holocene climate inferred from oxygen isotope ratios in lake sediments, Central Brooks Range, Alaska. *Quaternary Research* 55, 313–21.

Anderson, L., Abbott, M.B., Finney, B.P. and **Burns, S.J. 2005**: Regional atmospheric circulation change in the North Pacific during the Holocene inferred from lacustrine carbonate oxygen isotopes, Yukon Territory, Canada. *Quaternary Research* 64, 21–35.

Anderson, P.M. and **Brubaker, L.B.** 1994: Vegetation history of north-central Alaska: a mapped summary of late-Quaternary pollen data. *Quaternary Science Reviews* 13, 71–92.

Barber, V. and **Finney, B.P.** 2000: Late Quaternary paleoclimatic reconstructions for interior Alaska based on paleo lake-level data and hydrologic models. *Journal of Paleolimnology* 24, 29–41.

Bengtsson, L. and **Enell, M.** 1986: Chemical analyses. In Berglund, B.E., editor, *Handbook of Holocene paleoecology and paleohydrology.* Chichester: J. Wiley, 423–51.

Berger, A. and **Loutre, M.F.** 1991: Insolation values for the climate of the last 10 million years. *Quaternary Science Reviews* 10, 297–317.

Bigelow, N. and **Edwards, M.E.** 2001: A 14,000 yr paleoenvironmental record from Windmill Lake, Central Alaska: late glacial and Holocene vegetation in the Alaska Range. *Quaternary Science Reviews* 20, 203–15.

Brown, T.A., Nelson, D.E., Mathewes, R.W., Vogel, J.S. and **Southen, J.R.** 1989: Radiocarbon dating of pollen by accelerator mass spectrometry. *Quaternary Research* 32, 205–12.

Burn, C.R. 1997: Cryostratigraphy, paleogeography, and climate change during the early Holocene warm interval, western Arctic coast, Canada. *Canadian Journal of Earth Sciences* 34, 912–25.

Burn, C.R., Michel, F.A. and **Smith, M.W.** 1986: Stratigraphic, isotopic, and mineralogical evidence for an early Holocene thaw unconformity at Mayo, Yukon Territory. *Canadian Journal of Earth Sciences* 23, 794–803.

Calkin, P.E., Wiles, G.C. and **Barclay, D.J.** 2001: Holocene coastal glaciation of Alaska. *Quaternary Science Reviews* 20, 449–61.

Clague, J.J., Evans, S.G., Rampton, V.N. and **Woodsworth, G.J.** 1995: Improved age estimates for the White River and Bridge River tephras, western Canada. *Canadian Journal of Earth Sciences* 32, 1172–79.

Cwynar, L.C. 1988: Late Quaternary vegetation history of Kettlehole Pond, southwestern Yukon. *Canadian Journal of Forest Research* 18, 1270–79.
Cwynar, L.C. and **Spear, R.W.** 1991: Reversion of forest to tundra in the central Yukon. *Ecology* 72, 202–12.
—— 1995: Paleovegetation and paleoclimatic changes in the Yukon at 6 ka BP. *Geographie Physique et Quaternaire* 49, 29–35.
Dean, W.E. 1999: The carbon cycle and biogeochemical dynamics in lake sediments. *Journal of Paleolimnology* 21, 375–93.
Dean, W.E. and **Megard, R.O.** 1993: Environment of deposition of $CaCO_3$ in Elk Lake, Minnesota. In Bradbury, J.P. and Dean, W.E., editors, *Elk Lake, Minnesota: evidence for rapid climate change in the north-central United States.* Boulder CO: Geological Society of America Special Paper 276, 97–113.
Dean, W.E. and **Stuiver, M.** 1993: Stable carbon and oxygen isotope studies of the sediments of Elk Lake, Minnesota. In Bradbury, J.P. and Dean, W.E., editors, *Elk Lake, Minnesota: evidence for rapid climate change in the north-central United States.* Boulder CO: Geological Society of America Special Paper 276, 163–80.
Denton, G.H. and **Karlén, W.** 1977: Holocene glacial and tree-line variations in the White River Valley and Skolai Pass, Alaska and Yukon Territory. *Quaternary Research* 7, 63–111.
Digerfeldt, G. 1986: Studies on past lake level fluctuations. In Berglund, B.E., editor, *Handbook of Holocene paleoecology and paleohydrology.* Chichester: J. Wiley, 127–43.
Dyke, A.S., Andrews, J.T., Clark, P.U., England, J.H., Miller, G.H., Shaw, J. and **Veillette, J.J.** 2002: The Laurentide and Innuitian ice sheets during the Last Glacial Maximum. *Quaternary Science Reviews* 21, 9–31.
Edwards, M.E. and **Barker, E.D.** 1994: Climate and vegetation in northeastern Alaska 18,000 yr B.P. – present. *Palaeogeography, Palaeoclimatology, Palaeoecology* 109, 127–35.
Environment Canada 2003: *Canadian climate normals.* http://climate.weatheroffice.ec.gc.ca/climate_normals/index_e.html
Farnell, R., Hare, G.P., Blake, E., Bowyer, V., Schweger, C., Greer, S. and **Gotthardt, R.** 2004: Multidisciplinary investigations of alpine ice patches in southwest Yukon, Canada: paleoenvironmental and paleobiological investigations. *Arctic* 57, 247–59.
Fee, E.J., Hecky, R.E., Kasian, S.E.M. and **Cruikshank, D.R.** 1996: Effects of lake size, water clarity, and climatic variability on mixing depths in Canadian Shield lakes. *Limnology and Oceanography* 41, 912–20.
Finney, B.P., Edwards, M.E., Abbott, M.B., Barber, V., Anderson, L. and **Rohr, M.** 2000: Holocene precipitation variability in interior Alaska. *30th International Arctic Workshop Program and Abstracts.* Boulder CO: Institute for Arctic and Alpine Research, xvi, 60.
Fisher, D.A., Bourgeois, J., Demuth, M., Koerner, R.M., Parnandi, M., Sekerka, J., Zdanowicz, C., Zheng, J., Wake, C., Yalcin, K., Mayewski, P., Kreutz, C., Osterberg, E., Dahl-Jensen, D., Goto-Azuma, K., Holdsworth, G., Steig, E., Ruper, S. and **Wasckiewicz, M.** 2004: Mount Logan ice cores: the water cycle in the North Pacific in the Holocene. *EOS* 85, American Geophysical Union Fall Meeting Supplement, Abstract PP23C-07.
Heiri, O., Lotter, A.F. and **Lemcke, G.** 2001: Loss on ignition as a method for estimating organic and carbonate content in sediments: reproducibility and comparability of results. *Journal of Paleolimnology* 25, 101–10.
Hodell, D.A., Schelske, C.L., Fahnenstiel, G.L. and **Robbins, L.L.** 1998: Biologically induced calcite and its isotopic composition in Lake Ontario. *Limnology and Oceanography* 43, 187–99.
Kendal, C. 1998: Tracing nitrogen sources and cycling in catchments. In Kendal, C. and McDonnell, J.J., editors, *Isotope tracers in catchment hydrology.* Amsterdam: Elsevier, 519–76.
Lacourse, T. and **Gajewksi, K.** 2000: Late Quaternary history of black spruce and grasslands in southwest Yukon Territory. *Canadian Journal of Botany* 70, 1336–45.
Lamoreux, S. and **Cockburn, J.M.H.** 2005: Timing and climatic controls over Neoglacial expansion in the northern Coast Mountains, British Columbia. *The Holocene* 15, 619–24.
Lauriol, B., Grimm, W., Cabana, Y., Cinq-Mars, J. and **Geurtz, M.A.** 2001: Cliff-top eolian deposits as indicators of Late Pleistocene and Holocene Beringia. *Quaternary International* 87, 59–79.
Lauriol, B., Duduay, C.R. and **Riel, A.** 2002: Response of the Porcupine and Old Crow rivers in northern Yukon, Canada, to Holocene climatic change. *The Holocene* 12, 27–34.
Mackay, J.R. 1992: Lake stability in an ice-rich permafrost environment: examples from the western arctic coast. In Robarts, R.D. and Bothwell, M.L., editors, *Aquatic ecosystems in semi-arid regions: implications for resource management.* Symposium Series 7, Saskatoon: Environment Canada, 1–25.
Mann, D.H. and **Hamilton, T.D.** 1995: Late Pleistocene and Holocene paleoenvironments of the North Pacific coast. *Quaternary Science Reviews* 14, 449–71.
McConnaughy, T. 1991: Calcification in *Chara corallina*: CO_2 hydroxylation generates protons for bicarbonate assimilation. *Limnology and Oceanography* 36, 619–28.
McConnaughy, T.A., LaBaugh, J.W., Rosenberry, D.O. and **Streigel, R.G.** 1994: Carbon budget for a groundwater-fed lake: calcification supports summer photosynthesis. *Limnology and Oceanography* 39, 1319–32.
McKenzie, J.A. 1985: Carbon isotopes and productivity in the lacustrine and marine environment. In Stumm, W., editor, *Chemical processes in lakes.* Toronto: J. Wiley, 99–118.
Mock, C.J., Bartlein, P.J. and **Anderson, P.A.** 1998: Atmospheric circulation patterns and spatial climatic variations in Beringia. *International Journal of Climatology* 18, 1085–104.
Oana, S. and **Deevey, E.S.** 1960: Carbon-13 in lake waters and its possible bearing on paleolimnology. *American Journal of Science* 258-A, 253–72.
Pietnitz, R., Smol, J.P., Last, W.M., Leavitt, P.R. and **Cumming, B.F.** 2000: Multi-proxy Holocene paleoclimatic record from a saline lake in the Canadian subarctic. *The Holocene* 10, 673–86.
Ramisch, F., Ditrich, M., Mattenberger, C., Wehrli, B. and **Wüest, A.** 1999: Calcite dissolution in two deep eutrophic lakes. *Geochimica et Cosmochimica Acta* 63, 3349–56.
Ritchie, J.C. and **Harrison, S.P.** 1993: Vegetation, lake levels, and climate in western Canada during the Holocene. In Wright, H.E., Kutzbach, J.E., Webb, T., III, Ruddiman, W.F., Street-Perrott, F.A. and Bartlein, P.J., editors, *Global climate since the Last Glacial Maximum.* Minneapolis MN: University of Minnesota Press, 401–14.
Ritchie, J.C., Cwynar, L.C. and **Spear, R.W.** 1983: Evidence from north-west Canada for an early Holocene Milankovitch thermal maximum. *Nature* 305, 126–28.
Spooner, I.S., Barnes, S., Baltzer, K.B., Raeside, R., Osborn, G.D. and **Mazzuchi, D.** 2003: The impact of air mass circulation dynamics on late Holocene paleoclimate in northwestern North America. *Quaternary International* 108, 77–83.
Stabel, H-H. 1986: Calcite precipitation in Lake Constance: chemical equilibrium, sedimentation, and nucleation by algae. *Limnology and Oceanography* 31, 1081–93.
Stuart, S.L., Helmer, J.W. and **Hills, L.V.** 1989: The Holocene paleoecology of Jenny Lake area, southwest Yukon, and its implications for prehistory. *Arctic* 42, 347–53.
Stuiver, M., Reimer, P.J., Bard, E., Beck, J.W., Burr, G.S., Hughen, K.A., Kromer, B., McCormac, F.G., v.d.Plicht, J. and **Spurk, M.** 1998: Radiocarbon age calibration 24,000–0 cal BP. *Radiocarbon* 40, 1041–83.
Vardy, S.R., Warner, B.G. and **Aravena, R.** 1997: Holocene climate effects on the development of a peatland on the Tuktoyaktuk Peninsula, Northwest Territories. *Quaternary Research* 47, 90–104.
Wahl, H.E., Fraser, D.B., Harvey, R.C. and **Maxwell, J.B.** 1987: *Climate of the Yukon.* Ottawa: Climatic Studies by Environment Canada, Atmospheric Environment Service, 1–323.
Wang, X.-C. and **Geurts, M.-A.** 1991: Late Quaternary pollen records and vegetation history of the southwest Yukon Territory: a review. *Géographie Physique et Quaternaire* 45, 175–193.